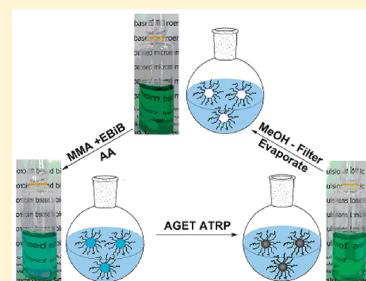


Low-Temperature AGET ATRP of Methyl Methacrylate in Ionic Liquid-Based Microemulsions

Yinxia Zhou,[†] Lihua Qiu,[†] Zhijun Deng,[†] John Texter,[‡] and Feng Yan^{*,†}[†]Jiangsu Key Laboratory of Advanced Functional Polymer Design and Application, Department of Polymer Science and Engineering, College of Chemistry, Chemical Engineering and Materials Science, Soochow University, Suzhou, 215123, P. R. China[‡]School of Engineering Technology, Eastern Michigan University, Ypsilanti, Michigan 48197, United States

S Supporting Information

ABSTRACT: Sustainable atom transfer radical polymerization of methyl methacrylate (MMA) with activators generated by electron transfer (AGET ATRP) was done using microemulsion polymerization at the relatively low temperature of 30 °C. Ethyl 2-bromoisobutyrate (EBiB) was used as ATRP initiator, ascorbic acid (AA) was used as reducing agent, and CuCl₂/N-bis(2-pyridylmethyl)octylamine (BPMOA) was used as catalyst. Microemulsion AGET ATRP of MMA was well-controlled, producing poly(methyl methacrylate) (PMMA) nanoparticles ~5 nm in diameter and narrow molecular weight distributions ($M_w/M_n = 1.20\text{--}1.40$). After the polymerization and isolation of PMMA, the mixture containing catalysts and ILs was shown to be recoverable and recyclable. Upon replenishment of initiator, reducing agent, and monomer (MMA), AGET ATRP of MMA produced PMMA with reproducible molecular weights and narrow molecular weight distributions, even in the fifth cycle. Thus, this process was demonstrated as being sustainable. Furthermore, use of a new surfactant IL ligand, 3-[11-[(3-(bis(pyridin-2-ylmethyl)amino)propanoyl)oxy]undecyl]-1-methylimidazolium bromide (BPYP-[MIM]Br) or 3-[11-[(3-(bis(pyridin-2-ylmethyl)amino)propanoyl)-oxy]undecyl]-1-methylimidazolium hexafluorophosphate (BPYP-[MIM]PF₆), demonstrated rate-enhanced polymerization relative to the use of BPMOA as ligand, and good polydispersity ($M_w/M_n = 1.20\text{--}1.50$) of the resultant PMMA was maintained.



■ INTRODUCTION

Microemulsions are transparent and thermodynamically stable isotropic dispersions containing nanosized domains stabilized by suitable surfactants.¹ They are homogeneous and isotropic at a macroscopic level and heterogeneous at molecular and supramolecular length scales. Since the early 1980s, microemulsion polymerization has developed rapidly as an important methodology for polymer synthesis of latexes and nanostructured polymers.² Both conventional free radical polymerization and controlled/"living" radical polymerization (CLRP)³ in microemulsions have been extensively studied. CLRP techniques, such as atom transfer radical polymerization (ATRP),⁴ nitroxide-mediated radical polymerization (NMP),⁵ reversible addition–fragmentation chain transfer (RAFT),⁶ and iodine-transfer polymerization (ITP)⁷ are powerful tools for the preparation of well-defined functional polymers with controlled molecular weights and narrow molecular weight distributions.

During the past decade, polymers with a variety of topologies and well-defined chain-end functionalities have been successfully prepared via CLRP techniques, either in bulk, solution, or heterogeneous media, mostly in oil-in-water heterogeneous systems, such as emulsions, miniemulsions, and microemulsions.^{1,3,4a,8,9} For instance, surface-functionalized nanostructured polymers, such as latexes, gels, and molecular brushes, have been successfully synthesized via microemulsion ATRP.¹⁰ However, one main

drawback of microemulsion ATRP is that a high concentration of transition-metal catalyst is generally required. These catalysts are easily coprecipitated with the polymer and may color the product and even make the polymers toxic. In addition, conventional microemulsion polymerization systems usually require a high concentration of surfactant to stabilize a relatively low amount of monomer. Therefore, postpolymerization purification often makes the work-up very tedious when trying to purify the resultant polymers.² In order to overcome this drawback, ATRP in ionic liquid-based microemulsions has recently been developed.^{10a}

Ionic liquids (ILs) are organic salts with melting points at or near room temperature. They have gained a great deal of both academic and industrial attention because of their low volatility, high stability, and high ion conductivity. IL-based microemulsions have recently attracted a great deal of interest because of their unique features of both ILs and microemulsions.¹⁰ It has been demonstrated that polymerizations, including free radical and CLRP in IL-based microemulsions, exhibit behavior consistent with that in "classic" water/oil microemulsions.¹⁰ For example, ATRP in IL-based microemulsions produced polymer

Received: July 7, 2011

Revised: August 30, 2011

Published: September 16, 2011

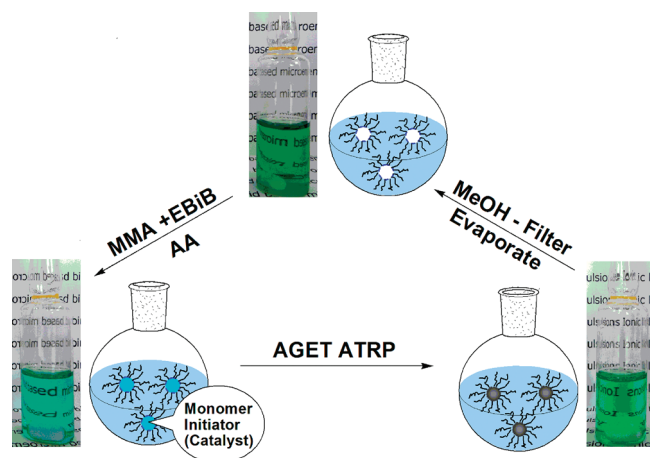


Figure 1. The starting microemulsion containing monomer, initiator, catalyst, surfactant, and [Bmim][BF₄] (bottom left) undergoes AGET ATRP to produce a suspension of polymer nanolatexes (bottom right); drowning in MeOH to precipitate the polymer nanolatexes, filtration to remove product, and evaporation leaves a micellar solution of surfactant in [Bmim][BF₄] (top center); addition of monomer, EBiB, and electron transfer (reducing) agent AA regenerates the microemulsion (lower left).

nanoparticles with narrow molecular weight distributions. After the polymerization and isolation of resultant polymers, a mixture containing catalyst, surfactant, and ILs can be recovered and reused. However, the catalyst (such as Cu(I) complex) used for normal ATRP is generally sensitive to air and humidity, which requires an aerobic processing and therefore not suitable for sustainable polymerizations. These limitations can be avoided by using activators generated by electron transfer ATRP (AGET ATRP) process, where the catalyst Cu(II) complex is not air-sensitive.

Herein, we report the first example of AGET ATRP of methyl methacrylate (MMA) in an IL-based microemulsion at 30 °C. Microemulsion AGET ATRP produced PMMA nanoparticles (~5 nm) with controlled molecular weights and narrow molecular weight distributions. Isolation of the resultant polymers and further addition of monomer (containing initiator and reducing agent) into the recovered IL mixture regenerates a microemulsion suitable for another polymerization cycle (Figure 1). In order to increase the polymerization rate, surfactant IL catalyst ligands, 3-{11-[(3-(bis(pyridin-2-ylmethyl)amino)propanoyl)oxy]undecyl}-1-methylimidazolium Br⁻ (BPYP-[MIM]Br) and 3-{11-[(3-(bis(pyridin-2-ylmethyl)amino)propanoyl)oxy]undecyl}-1-methylimidazolium PF₆⁻ (BPYP-[MIM]PF₆), were synthesized and showed rate-enhanced polymerization.

EXPERIMENTAL SECTION

Materials. Methyl methacrylate (MMA) (99%) was washed with an aqueous solution of sodium hydroxide (NaOH) (5 wt %) three times, followed by deionized water until neutralization, and then dried over anhydrous magnesium sulfate, distilled under reduced pressure, and stored at -18 °C. Copper(II) chloride dihydrate (CuCl₂) (99%), ascorbic acid (AA) (99%), *n*-butyl bromide, and tetrahydrofuran (THF) were purchased from Shanghai Chemical Reagents Co. (Shanghai, China) and used as received. Ethyl 2-bromoisobutyrate (EBiB) (98%), di(2-picoly)amine (95%), 2-(chloromethyl)pyridine hydrochloride (97%), 1-octylamine (99%), 1-bromododecane

(99%), 11-bromo-1-undecanol (97%), sodium tetrafluoroborate (NaBF₄) (98%), potassium hexafluorophosphate (KPF₆) (98%), methylimidazole (99%), and 2,2-bipyridine (Bipy) (95%) were purchased from Acros and used without further purification. *N,N,N',N',N'*-Pentamethyldiethylenetriamine (PMDETA) (95%) was purchased from Aldrich and used without further purification. 1-(2-Acryloyloxyundecyl)-3-methylimidazolium bromide (AMIBr) and surfactant 1-dodecyl-3-methylimidazolium bromide (DMIBr) were synthesized as reported in the literature.¹¹ Bis(2-pyridylmethyl)octylamine (BPMOA) was synthesized as described earlier by Xia and Matyjaszewski.¹²

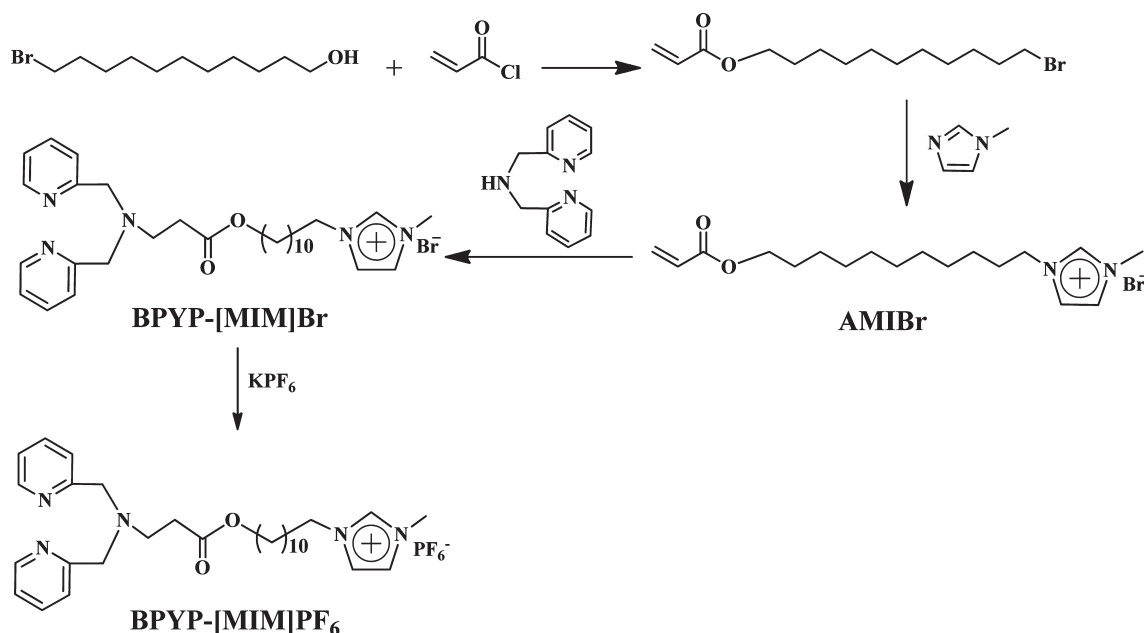
Synthesis of Ligand 3-{11-[(3-(Bis(pyridin-2-ylmethyl)amino)propanoyl)oxy]undecyl}-1-methylimidazolium Bromide (BPYP-[MIM]Br) (Scheme 1). A mixture of AMIBr (3.75 g, 12 mmol) and di(2-picoly)amine (2.40 g, 12 mmol) were dissolved in 10 mL of dry CH₂Cl₂ and stirred at 60 °C for 72 h.¹³ CH₂Cl₂ was evaporated, and the resultant viscous liquid was washed with diethyl ether and ethyl acetate twice and then dried in dynamic vacuum at room temperature to yield a yellow liquid: 4.86 g (79% yield). ¹H NMR (CDCl₃, 400 MHz) δ (ppm): 10.51 (s, 1H), 8.49 (d, 2H), 7.69 (s, 1H), 7.64 (m, 2H), 7.48 (d, 2H), 7.34 (s, 1H), 7.14 (t, 2H), 4.30 (t, 2H), 4.11 (s, 4H), 3.99 (t, 2H), 3.82 (s, 3H), 2.92 (t, 2H), 2.54 (t, 2H), 1.92 (m, 6H), 1.27 (m, 12H).

Synthesis of Ligand 3-{11-[(3-(Bis(pyridin-2-ylmethyl)amino)propanoyl)oxy]undecyl}-1-methylimidazolium hexafluorophosphate (BPYP-[MIM]PF₆) (Scheme 1). A solution of BPYP-[MIM]Br (5.298 g, 11.5 mmol) in water was added into adequate KPF₆ (3.173 g, 17.25 mmol) and stirred at room temperature for 48 h. The precipitate was washed with water and dried under vacuum at room temperature to give a yellow liquid: 5.15 g (85% yield). ¹H NMR (CDCl₃, 400 MHz) δ (ppm): 8.64 (s, 1H), 8.49 (d, 2H), 7.68 (s, 1H), 7.65 (m, 2H), 7.47 (d, 2H), 7.22 (s, 1H), 7.15 (t, 2H), 4.13 (t, 2H), 4.01 (t, 2H), 3.91 (d, 4H), 3.84 (s, 3H), 2.93 (t, 2H), 2.55 (t, 2H), 1.82 (m, 6H), 1.27 (m, 12H).

AGET ATRP of MMA in IL-Based Microemulsion. A solution containing surfactant 1-dodecyl-3-methylimidazolium bromide (DMIBr) (0.6 g, 1.8 mmol) and [Bmim][BF₄] (3.0 g, 13.7 mmol) was degassed by three freeze–pump–thaw cycles in vacuo and then stirred under a nitrogen atmosphere. A mixture of MMA (208 μ L, 2.05 mmol), EBiB (3.01 μ L, 0.0205 mmol), CuCl₂ (2.8 mg, 0.0205 mmol), and BPMOA (12.4 mg, 0.041 mmol) was stirred at room temperature for 2 h and then added to the DMIBr/[Bmim][BF₄] solution. This mixture was stirred at room temperature for 30 min to form a transparent solution (microemulsion). AA (1.8 mg, 0.01 mmol) was then added. The microemulsion was then degassed with N₂, and the polymerization was done at 30 °C under a nitrogen atmosphere. After the completion of the polymerization, the reaction was stopped by immersing in an ice bath and then drowning in methanol. The precipitated polymer was isolated by filtration, washed with methanol, and dried in a vacuum at 60 °C. After the evaporation of methanol and residue of unreacted MMA, AGET ATRP of MMA was carried out again in the recovered IL mixture after addition of MMA, EBiB, and AA.

Chain Extension of PMMA Using PMMA as a Macroinitiator. The PMMA sample ($M_{n, GPC}$ = 4100 g/mol, M_w/M_n = 1.25) obtained via microemulsion AGET ATRP with the molar ratio of [MMA]₀/[EBiB]₀/[CuCl₂]₀/[BPMOA]₀/[AA]₀ = 100/1/1/2/0.5 was used as a macroinitiator for the chain extension reaction. PMMA macroinitiator (21.1 mg, 0.0051 mmol) was dissolved in 1 mL of THF, and the AGET ATRP was conducted with the molar ratio of [MMA]₀/[PMMA]₀/[CuCl₂]₀/[BPMOA]₀/[AA]₀ = 100/0.25/1/2/0.5. The chain-extension reaction was carried out in THF under stirring at 60 °C. The monomer conversion was 61% by gravimetric calculation after 30 h. The M_n and M_w/M_n values were determined by GPC with PMMA standards. ($M_{n, GPC}$ = 14 600 g/mol, M_w/M_n = 1.10).

Scheme 1. Synthetic Route of Surfactant IL Ligands



Characterization. ^1H NMR spectra were recorded on a UNITY INOVA 400 MHz nuclear magnetic resonance instrument using CDCl_3 as the solvent and tetramethylsilane (TMS) as an internal standard. The number-average molecular weight (M_n) and molecular weight distribution (M_w/M_n) of the resulting polymers were obtained by a Waters 1515 gel permeation chromatograph (GPC) equipped with a refractive index detector (Waters 2414). THF was used as the eluent at a flow rate of 1.0 mL/min at 30 °C. Samples were injected using a Waters 717 plus autosampler, and the column was calibrated with polystyrene standards purchased from Waters. The residue copper concentration in the resultant polymers was measured by inductively coupled plasma (ICP) (Vista MPX). The polymer powder (50.0 mg) was dissolved in nitric acid with heating and was then diluted to 25 mL for ICP analysis. The dynamic light scattering (DLS) measurements were performed using a high-performance particle size HPPS 5001 autosizer (Malvern Instrument, U.K.). Transmission electron microscopy (TEM) characterization was performed on a JEOL JEM-2010 electron microscope operating at an acceleration voltage of 200 kV.

RESULTS AND DISCUSSION

Microemulsion AGET ATRP of MMA Using BPMOA/CuCl₂ as the Catalyst. Microemulsion AGET ATRP of MMA was conducted in a 1-butyl-3-methylimidazolium tetrafluoroborate ([Bmim][BF₄])-based microemulsion stabilized by 1-dodecyl-3-methylimidazolium bromide (DMIBr) at 30 °C. An [Bmim][BF₄]/DMIBr/MMA ternary phase diagram is illustrated in the Supporting Information (see Figure S1). Samples within the one-phase microemulsion region were transparent and stable.^{10a} After the addition of reducing agent, AA, the color of polymerization system changed from blue to blue-green and then to green in a few minutes, indicating that Cu(II) has been effectively reduced to Cu(I). No phase separation was observed and all the IL-based microemulsions kept essentially transparent throughout the polymerization, as shown in Figure 1.

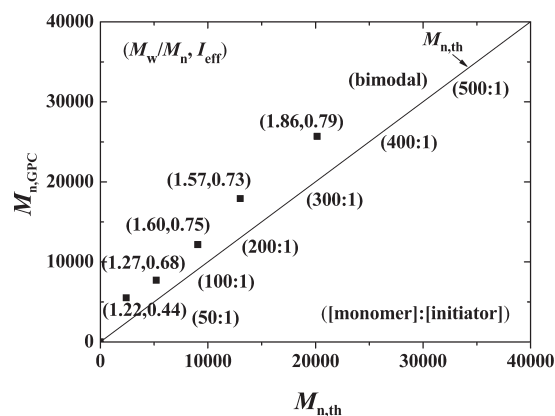


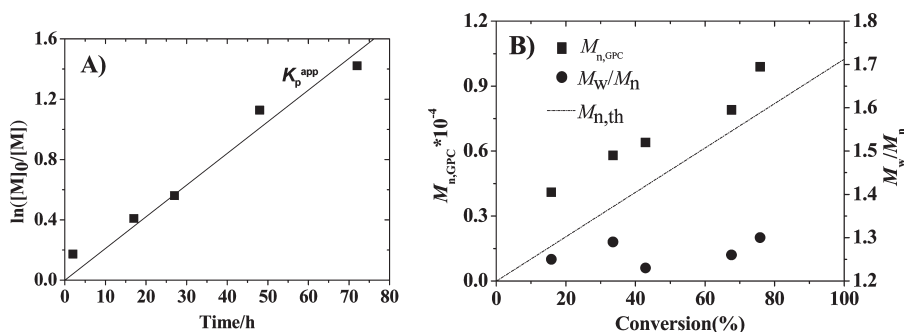
Figure 2. Relationship of molecular weight from GPC results ($M_{n,\text{GPC}}$) and theoretical molecular weight ($M_{n,\text{th}}$) under different molar feed ratios of $[\text{monomer}]_0/[\text{initiator}]_0$. $[\text{MMA}]_0/[\text{EBiB}]_0/[\text{CuCl}_2]_0/[\text{BPMOA}]_0/[\text{AA}]_0 = x/1/1/2/0.5$ ($x = 50, 100, 200, 300, 400, 500$). Polymerization temperature: 30 °C; time: 48 h; initiator efficiency ($I_{\text{eff}} = M_{n,\text{th}}/M_{n,\text{GPC}}$).

The effect of $[\text{MMA}]_0/[\text{EBiB}]_0$ on microemulsion AGET ATRP of MMA was first studied, and the results are summarized in Figure 2. It can be clearly seen that the molecular weight of polymers increased with the feed ratio of $[\text{MMA}]_0/[\text{EBiB}]_0$, while the molecular weight distributions (M_w/M_n) increased simultaneously. Under the circumstance of $[\text{MMA}]_0/[\text{EBiB}]_0$ was 50:1, PMMA with narrow molecular weight distributions ($M_w/M_n = 1.22$) was obtained, while the initiator efficiency of the polymerization was relatively low at 44%. When $[\text{MMA}]_0/[\text{EBiB}]_0$ was increased to 100:1, well-defined polymers with narrow molecular weight distribution ($M_w/M_n = 1.27$) at 64% conversion were obtained. However, as $[\text{monomer}]:[\text{initiator}]$ ratio increases further, the I_{eff} increases to 0.73–0.79 and the M_w/M_n increased to 1.86, and then a

Table 1. Effect of Ligands on AGET ATRP of MMA in IL-Based Microemulsions^a

entry	ligand	reaction time (h)	ligand solubility in [Bmim][BF ₄] (wt %)	conv (%)	$M_{n,th}$ (g/mol)	$M_{n,GPC}$ (g/mol)	M_w/M_n
1	Bipy	72	miscible				
2	PMDETA	72	22				
3	BPMOA	48	2.5	75.9	7590	9890	1.30

^a Polymerization conditions: [MMA]₀/[EBiB]₀/[CuCl₂]₀/[L]₀/[AA]₀ = 100/1/1/2/0.5; polymerization temperature: 30 °C.

**Figure 3.** (A) First-order rate plots and (B) dependence of M_n on the monomer conversion for the AGET ATRP of MMA conducted in IL-microemulsion at 30 °C. Conditions: [MMA]₀/[EBiB]₀/[CuCl₂]₀/[BPMOA]₀/[AA]₀ = 100/1/1/2/0.5.

bimodality in GPC traces was observed when the ratio of [MMA]₀/[EBiB]₀ was 500:1. This bimodality is what one usually observes in the free radical thermally initiated bulk polymerization of MMA as a result of the so-called gel effect. In this case the relative volume of [Bmim][BF₄]/MMA is about 0.67/0.62. If the latex particles formed were monodisperse, we would expect a very high viscosity, since the conversion/volume ratio is very close to the hard-sphere glass boundary at 49 particle (monomer) volume percent. The volume fraction of monomer at this ratio is 47.7%, and the volume fraction of PMMA, assuming complete conversion, would be in excess of 50%, in the glass domain. These results also indicate that microemulsion AGET ATRP of MMA polymerization is an efficient and well-controlled system at the relatively low feed ratio of [MMA]₀/[EBiB]₀ = 100:1.

For an efficiently active microemulsion AGET ATRP, a suitable ligand for the formation of catalyst complex is crucial for maintaining an appropriate equilibrium of activator and deactivator between the monomer oil-swollen micelles and the IL pseudocontinuous phase. Here, the effect of ligands including Bipy, PMDETA, and BPMOA on control over polymerization was investigated, and the results of polymerizations are summarized in Table 1. In the cases of two commercially available catalyst ligands, Bipy and PMDETA, no polymerization was observed. These results might be due to the high solubility of two catalyst ligands (Bipy/Cu(II) and PMDETA/Cu(II) complexes) in the [Bmim][BF₄] continuous phase. However, in the case of BPMOA, efficiently active polymerizations were obtained because the formed BPMOA/Cu(II) complex is nearly insoluble in [Bmim][BF₄] continuous phase. The reducing agent AA is highly soluble in these IL-based microemulsion and reduces the Cu(II) complexes either in the IL continuous phase or at the interface of monomer oil/IL droplets.^{1,9b} Upon the addition of AA, a reversible equilibrium of the activator BPMOA/Cu(I) and the deactivator BPMOA/Cu(II) in the monomer oil droplets is established, which provides an efficiently active polymerization.

Figure 3A shows the kinetic plots of microemulsion AGET ATRP of MMA with a molar ratio of [MMA]₀/[EBiB]₀/[CuCl₂]₀/[BPMOA]₀/[AA]₀ = 100/1/1/2/0.5. The linearity of the plot indicates that the polymerization is approximately first order with respect to the monomer concentration. The slope of the kinetic plots indicates that the number of active species was constant, and the termination reactions could be neglected throughout the polymerization process. The apparent rate constant (k_p^{app}) of polymerization catalyzed by BPMOA/CuCl₂, as determined from the kinetic slopes is $5.80 \times 10^{-6} \text{ s}^{-1}$. Figure 3B shows the evolution of the number-average molecular weight ($M_{n,GPC}$) and molecular weight distribution (M_w/M_n) values with monomer conversion in microemulsion AGET ATRP of MMA at 30 °C. The linearity of the plot indicated that the polymerization was approximately first order with respect to the monomer concentration and that the number of active species remained constant during the polymerization process, and the molecular weight distributions kept narrow ($M_w/M_n < 1.30$) even at high monomer conversion. These results indicated that the AGET ATRP of MMA in IL-based microemulsions can be an efficient radical polymerization process. However, the molecular weights of PMMA produced by BPMOA/CuCl₂ in IL-microemulsion were higher than theoretical values, indicating low initiator efficiency. Low initiation efficiency in IL-based microemulsion polymerizations might be due to two factors: First, the concentration of the deactivator was low in microemulsion, increasing primary radical termination in the oil phase. Second, the primary radicals might have diffused out of the oil droplets and terminated in the IL continuous phase.^{10f} These results are similar to the low initiator efficiency ($M_{n,GPC} > M_{n,th}$) of CLRP conducted in water–oil heterogeneous systems.^{14a,b,15} However, the increase in polydispersity with increasing monomer is most likely a gel effect due to increasing suspension viscosity as discussed above.

After the completion of polymerization, the reaction mixture was poured into a large amount of methanol. The precipitated

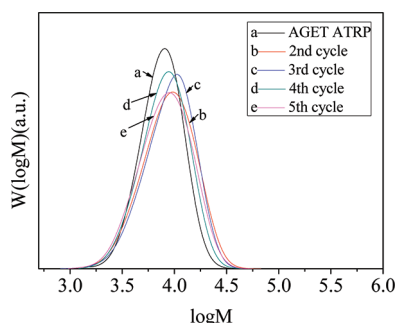


Figure 4. Typical GPC traces of the PMMA prepared via AGET ATRP in IL-based microemulsions using BPMOA/CuCl₂ as catalyst (as described in Table 2).

Table 2. AGET ATRP of MMA Conducted in IL-Based Microemulsions^a

entry	process	conv (%)	$M_{n,th}$ (g/mol)	$M_{n,GPC}$ (g/mol)	M_w/M_n
1	AGET ATRP	53.5	5350	7120	1.24
2	second cycle	61.4	6140	7920	1.38
3	third cycle	56.4	5640	8110	1.34
4	fourth cycle	60.8	6080	7380	1.30
5	fifth cycle	58.8	5880	7390	1.37

^a Polymerization conditions: [MMA]₀/[EBiB]₀/[CuCl₂]₀/[BPMOA]₀/[AA]₀ = 100/1/1/2/0.5; polymerization temperature: 30 °C; time: 40 h.

PMMA was isolated by filtration and washed with methanol. Since the surfactant DMIBr is miscible with [Bmim][BF₄] and methanol, it could be easily separated from the resultant polymers. After the evaporation of methanol and residual of unreacted monomer in vacuum, the IL mixture (containing surfactant and catalysts) was recovered. Addition of an appropriate amount of monomer (containing initiator and reducing agent) into the recovered IL mixture regenerated a transparent and stable microemulsion in which a second AGET ATRP cycle could be carried out. Although no extra catalyst, ligand, or surfactant was added, higher catalytic activity and similar control over polymerization were observed under the same experimental polymerization conditions. AGET ATRP of MMA in recovered IL-based microemulsions produced PMMA with reproducible molecular weights and narrow molecular weight distributions (Figure 4), even in the fifth cycle (Table 2). The copper residue concentration in the polymer produced was around 25 ppm determined by ICP-MS. DLS measurements show that the size of produced PMMA latex was ~6.7 nm in diameter (see Supporting Information, Figure S2), while TEM image shows that the particle size was ~5.9 nm. This small difference is due to the small particle polydispersity and the tendency of DLS measurements to exaggerate the contributions of the larger particles to the average size (Figure 5). These results also indicate that microemulsion polymerization at relatively low temperature (30 °C) could capture diameters close to those of droplet precursors.^{2a,b}

Effect of Ligands on the Polymerization Rate of MMA. Microemulsion AGET ATRP of MMA using BPMOA/CuCl₂ complexes as catalyst ligands produced PMMA nanoparticles with well to poorly controlled molecular weights and narrow to broad molecular weight distributions. In addition, the

polymerization rate ($k_p^{app} = 5.80 \times 10^{-6} \text{ s}^{-1}$) of such a microemulsion AGET ATRP needs to be improved. Therefore, surfactant IL consisting of an imidazolium cation polar group, a long carbon chain, and a di(2-picolyl)amine end group were synthesized and used as catalyst ligands for AGET ATRP. Scheme 1 shows the schematic synthesis of these surfactant IL ligands. A polymerizable IL surfactant 1-(11-acryloyloxyundecyl)-3-methylimidazolium bromide (AMIBr) was first synthesized as reported in the literature.¹¹ Michael addition reaction of the acryloyloxy group with di(2-picolyl)amine anchored the ligand onto the surfactant moiety and produced the ligand BPYP-[MIM]Br which is also a surfactant. Anion exchange of Br⁻ to PF₆⁻ yielded the surfactant ligand BPYP-[MIM]PF₆.

Figure 6A shows the kinetic plots of microemulsion AGET ATRP of MMA using BPYP-[MIM]Br/CuCl₂ or BPYP-[MIM]PF₆/CuCl₂ complexes as catalyst. The linearity of the plots indicates that both polymerizations are approximately first order with respect to the monomer concentration. The semilogarithmic plots of conversion are linear, and the molecular weights increase nearly linearly with conversion. Reasonably narrow molecular weight distributions ($M_w/M_n = 1.20\text{--}1.50$) were also obtained narrow (Figure 6B). Similarly to BPMOA/CuCl₂, molecular weights of PMMA produced by these surfactant IL ligand/CuCl₂ were much higher than theoretical values, probably due to the low initiation efficiency in IL-based microemulsion polymerizations.^{14c}

It should be noted that the polymerization rate (k_p^{app}) of BPYP-[MIM]Br/CuCl₂ and BPYP-[MIM]PF₆/CuCl₂ was calculated to be 1.50×10^{-5} and $1.36 \times 10^{-4} \text{ s}^{-1}$, respectively. Both are much higher than that of BPMOA/CuCl₂ ($k_p^{app} = 5.80 \times 10^{-6} \text{ s}^{-1}$). Compared with BPMOA/CuCl₂, which is highly soluble in monomer and nearly insoluble in IL continuous phase,^{10f} BPYP-[MIM]Br/CuCl₂ is a hydrophilic catalyst and nearly insoluble in monomer droplets while miscible with the [Bmim][BF₄] continuous phase. BPYP-[MIM]Br formulated from imidazole cations with appended carbon chains could act as surfactants in conventional imidazolium-based ILs, facilitating the emulsification of monomers within the IL continuous phases. Compared with BPMOA/CuCl₂ dissolved in monomer oil droplets, BPYP-[MIM]Br/CuCl₂ will distribute nearly homogeneously through the [Bmim][BF₄] IL continuous phase. Only a small fraction of the Cu(II) complex will reside in micellar cores. Consequently, a relatively higher ratio of [ascorbic acid]₀/[Cu(II)]₀ and lower concentrations of deactivator in the oil droplets resulted in a lower rate of deactivation and thereby resulted in a faster polymerization rate, slightly broader molecular weight distribution, and lower initiator efficiency than these of the BPMOA/CuCl₂ complex.^{14d} Furthermore, as a hydrophobic IL, BPYP-[MIM]PF₆ is miscible with both monomer oil and [Bmim][BF₄]. The BPYP-[MIM]PF₆/CuCl₂ complex, therefore, should be partly dissolved in both the monomer oil droplets and IL continuous phase, as well as in the oil droplet/IL interfacial layer. Addition of AA initiated polymerization quickly, and a reversible equilibrium of the activator and the deactivator was quickly established. The polymerization is faster and exhibited more efficient activity.

Microemulsion AGET ATRP of MMA catalyzed by BPYP-[MIM]Br is also recyclable (Table 3). A second AGET ATRP cycle was carried out upon the addition of a proper amount of monomer, initiator, and reducing agent. Higher catalytic activity and similar control over polymerization were observed in the

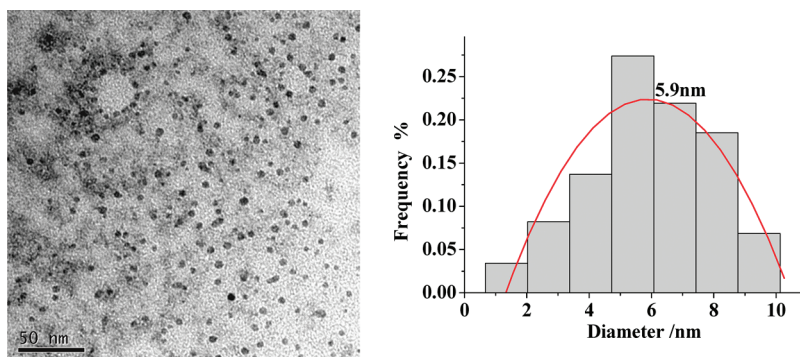


Figure 5. TEM images of PMMA latexes prepared via AGET ATRP in IL-based microemulsions. Polymerization conditions: $[MMA]_0/[EBiB]_0/[CuCl_2]_0/[BPMOA]_0/[AA]_0 = 100/1/1/2/0.5$. Polymerization temperature: 30 °C; time = 24 h.

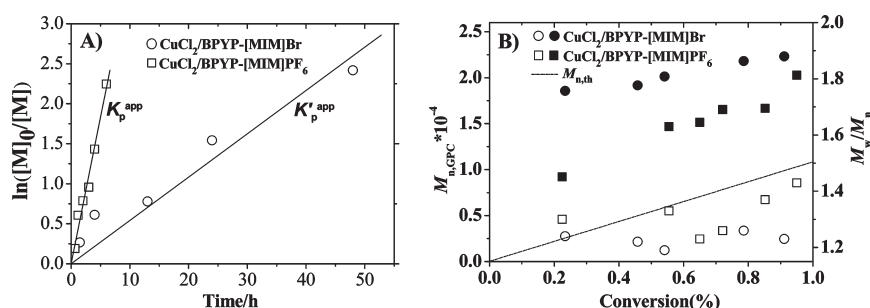


Figure 6. (A) First-order rate plots and (B) dependence of M_n on the monomer conversion for the AGET ATRP of MMA conducted in IL-microemulsion at 30 °C. Conditions: $[MMA]_0/[EBiB]_0/[CuCl_2]_0/[BPYP-[MIM]Br]_0$ (or $[BPYP-[MIM]PF_6]_0$)/ $[AA]_0 = 100/1/1/2/0.5$.

Table 3. AGET ATRP of MMA Conducted in IL-Based Microemulsions^a

entry	process	conv (%)	$M_{n,th}$ (g/mol)	$M_{n,GPC}$ (g/mol)	M_w/M_n
1	AGET ATRP	78.6	7860	21 810	1.26
2	second cycle	78.3	7830	18 440	1.34
3	third cycle	80.1	8010	15 620	1.48
4	fourth cycle	75.2	7520	20 540	1.37

^a Polymerization conditions: $[MMA]_0/[EBiB]_0/[CuCl_2]_0/[BPYP-[MIM]Br]_0/[AA]_0 = 100/1/1/2/0.5$; polymerization temperature: 30 °C.

subsequent cycles. AGET ATRP of MMA in recovered IL-based microemulsions produced PMMA with reproducible molecular weights and narrow molecular weight distributions ($M_w/M_n = 1.20–1.50$) (Figure 7). The copper residue concentration in the resultant PMMA was around 21 ppm determined by ICP-MS. Figure 8 shows the TEM image of PMMA latexes produced via AGET ATRP in IL-based microemulsions using BPYP-[MIM]Br/ $CuCl_2$ as the catalyst. PMMA latexes with an average diameter of ~ 4.2 nm and a narrow size distribution were obtained. The results of DLS measurements (~ 5.1 nm) strongly support the TEM results (see Supporting Information, Figure S3).

Analysis of Chain End and Chain Extension. Figure 9 shows the 1H NMR spectroscopy of the PMMA prepared via microemulsion AGET ATRP catalyzed by BPMOA/ $CuCl_2$. Signals at 4.10, 3.78, and 3.61 ppm were attributed to the protons of the methylene protons of the ethyl ester unit in the initiator EBiB

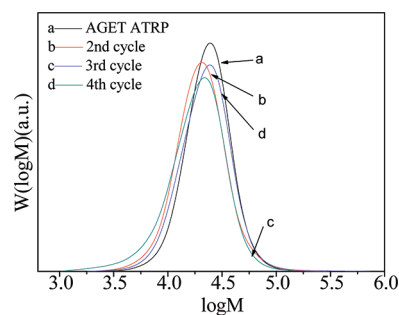


Figure 7. Typical GPC traces of PMMA synthesized via AGET ATRP in a $[Bmim][BF_4]$ -based microemulsion using $CuCl_2$ /BPYP-[MIM]Br as catalyst (as described in Table 3).

(peak a), the methyl ester group at the chain end (peak b), and the other methyl ester group in PMMA (peak c), respectively. The chemical shift at $\delta = 4.10$ (peak a) is attributed to the initiator EBiB moieties attached to the polymer chain ends. The peak c was associated with the methyl ester group at the chain end, which deviated from the chemical shift (3.61 ppm, peak b) of other methyl ester group in PMMA because of the electron-attracting function of the ω -Cl.¹⁶ Here, chain extension reactions were conducted using the synthesized PMMA ($M_{n,GPC} = 4100$ g/mol, $M_w/M_n = 1.25$) as a macroinitiator for the chain-extension experiment. Chain extended PMMA with $M_{n,GPC} = 14 600$ g/mol, $M_w/M_n = 1.10$ was produced as evidenced by GPC, as shown in Figure 10. The successful chain-extension reaction further verified the features of

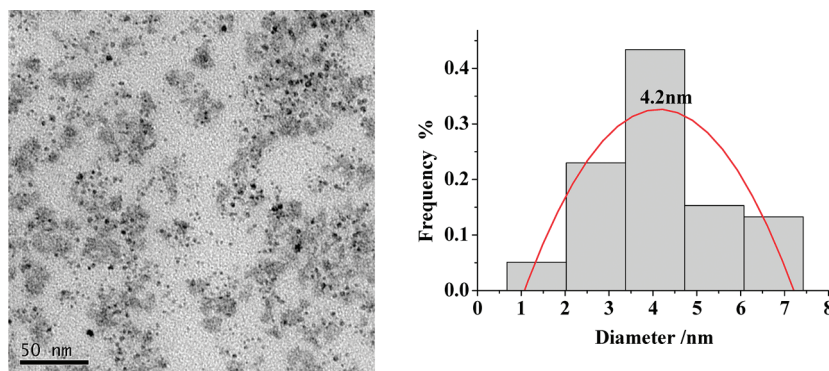


Figure 8. TEM images of PMMA latexes prepared via AGET ATRP in an IL-based microemulsion. Polymerization conditions: $[MMA]_0/[EBiB]_0/[CuCl_2]_0/[BPYP-[MIM]Br]_0/[AA]_0 = 100/1/1/2/0.5$; polymerization temperature: 30 °C; time: 24 h.

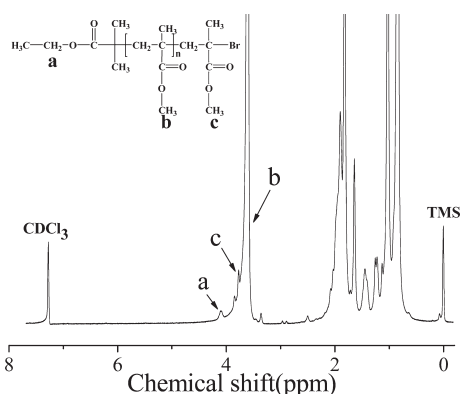


Figure 9. 1H NMR spectrum of PMMA ($M_{n,GPC} = 8320$ g/mol, $M_w/M_n = 1.27$) obtained via AGET ATRP in IL-based microemulsions with $CDCl_3$ as solvent and tetramethylsilane (TMS) as internal standard. Polymerization conditions: $[MMA]_0/[EBiB]_0/[CuCl_2]_0/[BPMOA]_0/[AA]_0 = 100/1/1/2/0.5$. Polymerization temperature: 30 °C; time: 48 h.

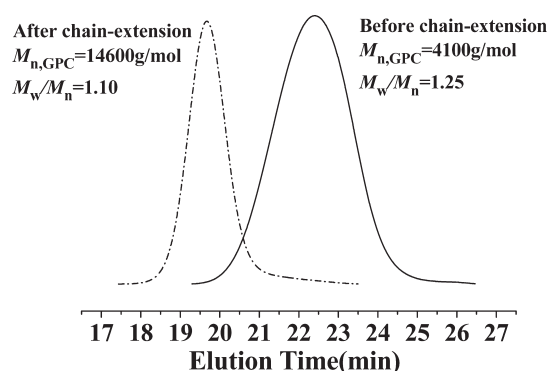


Figure 10. GPC curves before and after chain extension with PMMA as macroinitiator. Original PMMA prepared via AGET ATRP in IL-based microemulsion ($[MMA]_0/[EBiB]_0/[CuCl_2]_0/[BPMOA]_0/[AA]_0 = 100/1/1/2/0.5$); polymerization temperature: 30 °C; time: 12 h. Chain extended polymerization conditions: $[MMA]_0/[PMMA]_0/[CuCl_2]_0/[BPMOA]_0/[AA]_0 = 100/0.25/1/2/0.5$, 1 mL of THF as solvent; polymerization temperature: 60 °C; time: 30 h; conversion = 61%.

controlled/“living” free-radical polymerization of MMA in microemulsion AGET ATRP.

CONCLUSIONS

In summary, we have presented the first examples of microemulsion AGET ATRP of MMA in oil/IL ($MMA/[Bmim][BF_4]$) microemulsions initiated with $EBiB/AA/CuCl_2$ /ligand at low temperature (30 °C). After the polymerization and isolation of the PMMA, the mixture containing catalyst and ILs was recovered and reused. Addition of monomer to the recovered IL mixtures regenerated stable microemulsions that are ready for the next polymerization cycle upon addition of initiator and reducing agent. This process was demonstrated, thereby illustrating another example of IL-based sustainability in polymer synthesis.^{10a} Surfactant IL catalyst ligands, $BPYP-[MIM]Br$, and $BPYP-[MIM]PF_6$ show rate-enhanced polymerization. The method reported here combines the advantages of IL recycling and microemulsion polymerization. An unexpected but very significant result is the very small particle size ranges obtained (~ 5 nm diameter) with narrow molecular weight distributions ($M_w/M_n = 1.20$ – 1.50). The results of this study suggest a feasible approach for the practical applications of AGET ATRP in microemulsions and should be expected to promote the widespread use of CLRP techniques.

ASSOCIATED CONTENT

S Supporting Information. Characterization of microemulsion and polymer latex. This material is available free of charge via the Internet at <http://pubs.acs.org>.

AUTHOR INFORMATION

Corresponding Author

*E-mail: fyan@suda.edu.cn.

ACKNOWLEDGMENT

This work was supported by Natural Science Foundation of China (Nos. 20874071, 20974072, and 21174102), Research Fund for Ph.D. Programs Foundation of Ministry of Education of China (20103-201110003), and a Project Funded by the Priority Academic Program Development of Jiangsu Higher Education Institutions. We thank Prof. Z. Cheng, Prof. Z. Zhang, and Mr. L. Bai for helpful discussions.

REFERENCES

- (1) Min, K.; Matyjaszewski, K. *Macromolecules* **2005**, *38*, 8131–8134.
- (2) (a) Yan, F.; Texter, J. *Soft Matter* **2006**, *2*, 109–118. (b) Chow, P. Y.; Gan, L. M. *Adv. Polym. Sci.* **2005**, *175*, 257–298. (c) Co, C. C.;

de Vries, R.; Kaler, E. W. In *Reactions and Syntheses in Surfactant Systems*; Texter, J., Ed.; Marcel Dekker: New York, 2001; pp 455–469.

(3) (a) Zetterlund, P. B.; Kagawa, Y.; Okubo, M. *Chem. Rev.* **2008**, *108*, 3747–3794. (b) Cunningham, M. F. *Prog. Polym. Sci.* **2008**, *33*, 365–398. (c) Cunningham, M. F. *Prog. Polym. Sci.* **2002**, *27*, 1039–1067. (d) Qiu, J.; Charleux, B.; Matyjaszewski, K. *Prog. Polym. Sci.* **2001**, *26*, 2083–2134.

(4) (a) Min, K.; Gao, H.; Matyjaszewski, K. *J. Am. Chem. Soc.* **2006**, *128*, 10521–10526. (b) Kagawa, Y.; Kawasaki, M.; Zetterlund, P. B.; Okubo, M. *Macromol. Rapid Commun.* **2007**, *28*, 2354–2360. (c) Zetterlund, P. B.; Kagawa, Y.; Okubo, M. *Macromolecules* **2009**, *42*, 2488–2496.

(5) (a) Wakamatsu, J.; Kawasaki, M.; Zetterlund, P. B.; Okubo, M. *Macromol. Rapid Commun.* **2007**, *28*, 2346–2353. (b) Zetterlund, P. B.; Nakamura, T.; Okubo, M. *Macromolecules* **2007**, *40*, 8663–8672.

(6) Liu, S. Y.; Hermanson, K. D.; Kaler, E. W. *Macromolecules* **2006**, *39*, 4345–4350.

(7) Apostolo, M.; Arcella, V.; Storti, G.; Morbidelli, M. *Macromolecules* **2002**, *35*, 6154–6166.

(8) (a) Matyjaszewski, K.; Ziegler, M. J.; Arehart, S. V.; Greszta, D.; Pakula, T. *J. Phys. Org. Chem.* **2000**, *13*, 775–786. (b) Coessens, V.; Pintauer, T.; Matyjaszewski, K. *Prog. Polym. Sci.* **2001**, *26*, 337–377. (c) Davis, K. A.; Matyjaszewski, K. *Adv. Polym. Sci.* **2002**, *159*–169. (d) Moad, G.; Chong, Y. K.; Postma, A.; Rizzardo, E.; Thang, S. H. *Polymer* **2005**, *46*, 8458–8468. (e) Hidetaka Tobita. *Macromol. Theory Simul.* **2007**, *16*, 810–823.

(9) (a) Gaynor, S. G.; Qiu, J.; Matyjaszewski, K. *Macromolecules* **1998**, *31*, 5951–5954. (b) Min, K.; Gao, H. F.; Matyjaszewski, K. *J. Am. Chem. Soc.* **2005**, *127*, 3825–3830. (c) Airaud, C.; Ibarboure, E.; Gaillard, C.; Heroguez, V. *J. Polym. Sci., Part A: Polym. Chem.* **2009**, *47*, 4014–4027.

(10) (a) Chen, Z. Z.; Yan, F.; Qiu, L. H.; Lu, J. M.; Zhou, Y. X.; Chen, J. X.; Tang, Y. S.; Texter, J. *Langmuir* **2010**, *26*, 3803–3806. (b) Gao, H. X.; Li, J. C.; Han, B. X.; Yan, D. D. *Phys. Chem. Chem. Phys.* **2004**, *6*, 2914–2916. (c) Eastoe, S.; Gold, S. E.; Rogers, A.; Paul, T.; Welton, R. K.; Heenan, I. G. *J. Am. Chem. Soc.* **2005**, *127*, 7302–7303. (d) Qiu, Z. M.; Texter, J. *J. Curr. Opin. Colloid Interface Sci.* **2008**, *13*, 252–262. (e) Lu, J.; Yan, F.; Texter, J. *Prog. Polym. Sci.* **2009**, *34*, 431–448. (f) Li, N.; Gao, Y. A.; Zheng, L. Q.; Zhang, J.; Yu, L.; Li, X. W. *Langmuir* **2007**, *23*, 1091–1097.

(11) Yan, F.; Texter, J. *Chem. Commun.* **2006**, 2696–2698.

(12) Xia, J.; Matyjaszewski, K. *Macromolecules* **1999**, *32*, 2434–2437.

(13) Ding, S. J.; Radosz, M.; Shen, Y. Q. *Macromolecules* **2005**, *38*, 5921–5928.

(14) (a) Matyjaszewski, K.; Qiu, J.; Tsarevsky, N. V.; Charleux, B. *J. Polym. Sci., Part A: Polym. Chem.* **2000**, *38*, 4724–4734. (b) Jousset, S. P.; Qiu, J.; Matyjaszewski, K. *Macromolecules* **2001**, *34*, 6641–6648. (c) Kagawa, Y.; Zetterlund, P. B.; Minami, H.; Okubo, M. *Macromolecules* **2007**, *40*, 3062–3069. (d) Zhang, L.; Cheng, Z.; Lu, Y.; Zhu, X. *Macromol. Rapid Commun.* **2009**, *30*, 543–547.

(15) (a) Zetterlund, P. B.; Wakamatsu, J.; Okubo, M. *Macromolecules* **2009**, *42*, 6944–6952. (b) Matyjaszewski, K.; Qiu, J.; Shipp, D. A.; Gaynor, S. G. *Macromol. Symp.* **2000**, *155*, 15–29.

(16) (a) Audo, T.; Kamigaito, M.; Sawamoto, M. *Macromolecules* **1997**, *30*, 4507–4510. (b) Cheng, Z. P.; Zhu, X. L.; Chen, G. J.; Xu, W. J.; Lu, J. M. *J. Polym. Sci., Part A: Polym. Chem.* **2002**, *40*, 3823–3834.